

CHAPTER III

RESEARCH METHODOLOGY

3.1 A multiscale molecular simulations for structural and material properties of two polymer hosts for gel electrolytes of poly(vinyl chloride) : PVC and poly(vinyl fluoride) : PVF

Simulations to generate and equilibrate amorphous PVC and PVF structures were first done using the coarse-grained chains mapped on a high coordination lattice which was created by removing every other position from a diamond lattice, namely the 2nd nearest neighbor diamond (*2nnd*) lattice, with a coordination number of $10i^2 + 2$ at shell *i*th. All the coarse-grained bonds have the same length of 2.5 Å and the occupied lattice sites is 20.75%. For this reason, the simulation proficiency is the extremely developed comparison with MD simulation of atomistic model. The most essential characteristic is that polymer chains on *2nnd* lattice can be conveniently transformed to fully atomistic models and effectively recovered the real chain conformation. Moreover, the stereochemical structure of coarse-grained polymer chain can also be retained on the *2nnd* lattice which permit us to study the effect of side chain tacticity on structural properties of vinyl polymers from the on-lattice models as well.

3.1.1 Rotational Isomeric State (RIS) Model

RIS analysis is useful in conformational characterization of polymer molecules. This method is based on statistical thermodynamics to determine the average properties of ensemble derived from various different conformation according to its energetics. RIS model employs a small segment, usually dimer, to calculate for statistical weight matrices for each polymer conformation and then employ matrix multiplication scheme to determine the average conformational dependent properties. In the RIS scheme, the conformational partition function may be written as

$$Z = \sum_{\phi_1} \dots \sum_{\phi_n} e^{[-E(\phi_1 \dots \phi_n)/RT]} \quad (3.1)$$

For most polymer chains, this is a bad estimate because the state of a bond is influenced by the states of its neighbors. This is due to the pentane effect or the second-order interaction, named after the smallest molecule in which the phenomenon occurs. When taking into account the dependency of the nearest neighbor, the weight participatory with a given conformation is

$$\prod_i e^{[-E(\phi_{i-1}, \phi_i)RT]} \quad (3.2)$$

where $E_i(\phi_i)$ single bond energy, independent of the states of all other bonds. The statistical weight of the conformational state for each bond pair is given by

$$u_i(\phi_{i-1}, \phi_i) = e^{[-E(\phi_{i-1}, \phi_i)RT]} \quad (3.3)$$

The partition function can then be expressed as the sum over all rotational states of the product of these weights. That is

$$Z = \sum_{\phi_1} \dots \sum_{\phi_n} \prod_i u_i(\phi_{i-1}, \phi_i) \quad (3.4)$$

In matrix form, this can be rewritten as

$$Z = \prod_i U_i \quad (3.5)$$

where U_i is the statistical weight matrice of bond i .

It is constructive to consider the relative conformational energies for the model compounds of a polymer chain to be the sum of conformation-dependent interaction depending on single torsions (first-order) and consecutive pairs of torsions (second-order). Such RIS analysis is useful in understanding more conformational-dependent

interactions in these molecules. The quantities of interest in this work are the $\langle r^2 \rangle_0$, the $\langle r^2 \rangle_0 / nl^2$, $\langle s^2 \rangle_0 / nl^2$, and the fraction of bond conformer, all were tested to verify the characteristics of the polymer. Some of the useful mathematical formulas based on the original framework of the RIS model are listed below.

For example, the for the chain is obtained by evaluating the following matrix multiplication scheme.

$$\langle r^2 \rangle_0 = Z^{-1} G_1 \langle G_2 \rangle \cdots \langle G_{n-1} \rangle G_n \quad (3.6)$$

where Z is the conformational partition function.

U is the statistical weight matrices in the form as shown in Eq. (3.5).

$\langle \dots \rangle$ is the ensemble average for all possible conformations.

$$\langle G_i \rangle = \begin{bmatrix} U & (U \otimes I^T) \| T \| & 0 \\ 0 & (U \otimes I^T) \| T \| & U \otimes I \\ 0 & 0 & U \end{bmatrix}_i \quad (3.7)$$

G_i is the super generator matrix, I denotes to the identity matrix and \otimes denotes to the direct product. If U_i is of dimensions $\mathbf{V}_{i-1} \times \mathbf{V}_i$ and I_A is of dimensions 4×4 , the direct product, in the sequence $U_i \otimes I_A$, is of dimensions $4\mathbf{V}_{i-1} \times 4\mathbf{V}_i$, with the form

$$U_i \otimes I_A = \begin{bmatrix} u_{11} I_A & u_{12} I_A & \cdots \\ u_{21} I_A & u_{22} I_A & \cdots \\ \vdots & \vdots & \ddots \end{bmatrix} \quad (3.8)$$

T is the transformation matrix of the form

$$T_i = \begin{bmatrix} -\cos \theta & \sin \theta & 0 \\ -\sin \theta \cos \varphi & -\cos \theta \cos \varphi & -\sin \varphi \\ -\sin \theta \sin \varphi & -\cos \theta \sin \varphi & \cos \varphi \end{bmatrix} \quad (3.9)$$

where θ and φ denote the bond angle and the torsion angle, respectively.

Properties depend on other conformational such as $\langle s^2 \rangle_0 / nl^2$, and the fraction of bond conformer are calculated in the same way by changing only the super generator matrix for each of these properties.

3.1.2 RIS model of vinyl polymers

For example, the RIS model for vinyl- $[\text{CH}_2\text{-CH(X)}]_n$ - chains, where all bonds are subject to a torsion potential 3-fold asymmetry with the nearest neighbor interdependence. Determined by a statistical weight matrix for successive bonds of C-C^α and $\text{C}^\alpha\text{-C}$. Describing the stereochemistry with dl pseudo-asymmetric centers, the statistical weight matrix for the $\text{C}^\alpha\text{-C}$ and $\text{C}^\alpha\text{-C}$ bond are

$$U_d = \begin{bmatrix} \eta & 1 & \tau \\ \eta & 1 & \tau\omega \\ \eta & \omega & \tau \end{bmatrix} \quad (3.10)$$

when the methyl group is attached to C^α to produce a d pseudo-asymmetric center. The statistical weight matrices for the C-C^α bonds depend on the stereochemistry at two successive pseudo-asymmetric centers,

$$U_{dd} = \begin{bmatrix} \eta\omega_{xx} & \tau\omega_x & 1 \\ \eta & \tau\omega_x & \omega \\ \eta\omega_x & \tau\omega\omega_{xx} & \omega_x \end{bmatrix} \quad (3.11)$$

$$U_{dl} = \begin{bmatrix} \eta & \omega_x & \tau\omega_{xx} \\ \eta\omega_x & 1 & \tau\omega \\ \eta\omega_{xx} & \omega & \tau\omega_x^2 \end{bmatrix} \quad (3.12)$$

For an l pseudo-asymmetric center, the statistical weight matrices for these bonds become

$$U_l = QU_dQ, U_{ll} = QU_{dd}Q \text{ and } U_{ld} = QU_{dl}Q \quad (3.13)$$

$$\text{where } Q = \begin{bmatrix} 1 & 0 & 0 \\ 0 & 0 & 1 \\ 0 & 1 & 0 \end{bmatrix}$$

In these matrices, the states of bonds $i-1$ and i are denoted by the rows and columns, respectively, with t , g^+ , and g^- conformation. The *gauche* $\text{CH}\dots\text{CH}_3$ conformer is the reference state. The first-order energy E_η is a bond conformation with $\text{CH}\dots\text{X}$ in *gauche* interaction but not for $\text{CH}\dots\text{CH}_3$, while the other first-order energy, E_τ is a

conformation with both CH...X and CH...CH₃ in *gauche* interaction. E_ω is the second-order energy for CH₃...CH₃ “pentane” effect. E_{ω_x} and $E_{\omega_{xx}}$ are the second-order energies for CH₃...X and X...X interaction, respectively. In this work, the calculated conformational energies of small molecules, dichloroethane (DCE) and difluoroethane (DFE) respectively to represent PVC and PVF chains, based on *ab initio* electronic structure calculation at HF/6-311++G**//MP2/6-311++G** are reported in Table 4.1.1 and the RIS energies are determined for PVC and PVF chains are reported in Table 4.1.2 and 4.1.3 as: $E_\tau = -2.09$, $E_\eta = -3.76$, $E_\omega = 7.52$, $E_{\omega'} = 5.85$, $E_{\omega''} = 20.06$ kJ/mol $E_\tau = 3.51$, $E_\eta = -1.84$, $E_\omega = 7.19$, $E_{\omega'} = 2.51$, $E_{\omega''} = 13.63$ kJ/mol, respectively.

3.1.3 RIS parameters by quantum chemistry calculation

In an effort to quantify better the conformational energetics of vinyl polymers, *ab initio* electronic structure calculations will be performed to calculate geometries and conformational energetics for numerous stereoisomers of dimers. The parameterization of RIS model which more accurately conformational energies of model molecules can be obtained.

For a molecule in any particular conformation, one writes down the electronic Hamiltonian after the Born-Oppenheimer approximation as

$$H = \frac{-\hbar^2}{8\pi^2m} \sum_p \nabla_p^2 - \sum_A \sum_p e^2 Z_A r_{Ap}^{-1} + \sum_{p<q} \sum e^2 r_{pq}^{-1} \quad (3.14)$$

The total energy of the system is obtained as the sum of electronic energy and the nuclear repulsion energy. The electronic energy is the expectation value $\langle \psi | H | \psi \rangle$ where ψ is the wave function for the system obtained from the solution of the time-independent Schrodinger equation. For a closed shell system with $2n$ electrons, one can write ψ in the form

$$\psi = N \sum_p (-1)^p P \{ \psi_1(1)\alpha(1)\psi_1(2) \dots \psi_n(2n)\beta(2n) \} \quad (3.15)$$

where y_i are molecular orbitals and P is a permutation of the electron numbers a and b represent the spin of the electron involved.

Now the Hamiltonian can be divided into one- and two-electron parts. In terms of atomic units we have

$$H = H_1 + H_2 \quad (3.16)$$

where $H_1 = \sum_p H^{core}(p)$ with $H^{core}(p) = -\frac{1}{2} \nabla_p^2 - \sum_A Z_A r_{pA}^{-1}$ is the one-electron Hamiltonian corresponding to the motion of an electron in the field of the bare nuclei and $H_2 = \sum_{p < q} \sum r_{pq}^{-1}$. Then we get the total electronic energy as

$$E = 2 \sum_i^n H_{ii} + \sum_i^n \sum_j^n (2J_{ij} - K_{ij}) \quad (3.17)$$

where

$$\begin{aligned} H_{ii} &= \int \psi_i^*(1) H^{core} \psi_i(1) d\tau_1 \\ J_{ij} &= \int \int \psi_i^*(1) \psi_j^*(2) \frac{1}{r_{12}} \psi_i(1) \psi_j(2) d\tau_1 d\tau_2 \quad (\text{Coulomb integral}) \\ K_{ij} &= \int \int \psi_i^*(1) \psi_j^*(2) \frac{1}{r_{12}} \psi_j(1) \psi_i(2) d\tau_1 d\tau_2 \quad (\text{Exchange integral}) \end{aligned}$$

The optimal value of E is the energy that issues in the lowest energy for that particular conformation of the molecule. Thus, one can apply the variable essential and be able to adjust the molecular orbital until the energy decreases. In veritable operate, we demonstrate a molecular orbital as a linear combination of atomic orbitals (LCAO) as $\psi_i = \sum_\mu C_{\mu i} \varphi_\mu$. Furthermore, the properties of orthonormality imply that $\sum_{\mu\nu} C_{\mu i}^* C_{\nu j} S_{\mu\nu} = \delta_{ij}$ where $S_{\mu\nu} = \int \varphi_\mu(1) \varphi_\nu(1) d\tau_1$ and the density matrix is defined as $P_{\mu\nu} = 2 \sum_i^{occ} C_{\mu i}^* C_{\nu i}$. Eventually, the whole energy of the molecule can be indicated as

$$E = \sum_{\mu p} P_{\mu p} H_{\mu p} + \frac{1}{2} \sum_{\mu\nu\lambda\sigma} P_{\mu\nu} P_{\lambda\sigma} \left[(\mu\nu|\lambda\sigma) - \frac{1}{2} (\mu\lambda|\nu\sigma) \right] \quad (3.18)$$

where

$$\begin{aligned} H_{\mu\nu} &= \int \varphi_\mu^*(1) H^{core} \varphi_\nu(1) d\tau_1 \\ (\mu\nu|\lambda\sigma) &= \int \int \varphi_\mu^*(1) \varphi_\nu^*(1) \frac{1}{r_{12}} \varphi_\lambda(1) \varphi_\sigma(2) d\tau_1 d\tau_2 \end{aligned}$$

Now the variational principle can be used to minimize the energy; than one ends up with the equations

$$\sum_v (F_{\mu v} - \varepsilon_i S_{\mu v}) C_{vi} = 0 \quad (3.19)$$

where

$$F_{\mu v} = H_{\mu v} + \sum_{\lambda \sigma} P_{\lambda \sigma} \left[(\mu v | \lambda \sigma) - \frac{1}{2} (\mu \lambda | v \sigma) \right]$$

This equation was first set forth by Roothaan and is known as Roothaan equation. The series of coefficients must be regularly resolved in order to acquire the final eigenfunctions and the energy.

The SCF process relates to the selection of atomic orbitals from which the density matrices are calculated by employing some arbitrary value of C_{vi} . Then one solves the above equation to get new values of C_{vi} which will again be used in the above equation. This is repeated until the value of C_{vi} are self-consistent. This is known as Roothaan-Hartree-Fock procedure. In this work, we will use Gaussian09 computer program, which passed the above procedure self-consistently. Both use a combination of Gaussian functions as the input atomic functions. The only other input is the geometry of the molecule in particular configuration. The program will then observe the best energy for that situation.

For ab initio calculations, various geometries of low energy conformers of the stereoisomers of vinyl polymer dimers along with rotational energy barriers between the low-energy conformers were determined at the self-consistent-field (SCF) level using a 6-311++G** basis set, a 6-31G split-valence basis set plus polarization functions on all atoms. The geometry of all conformers is determined by fully optimizing the molecular geometries using the ab initio quantum chemistry package Gaussian03 which performs full geometry optimizations. The Hartree-Fock or SCF calculations exclude contributions from electron correlation. For conformational energy studies, the most significant participator to electron correlation effects is the dispersion energy which can be that can be calculated sufficiently through the use of second-order Moller-Plesset perturbation theory (MP2). Therefore, the SCF optimized geometries was used to calculate the MP2 level calculations of electron correlation effects. The single-point MP2 calculations were also operated using Gaussian03. The conformational geometries and energies of the difluoropentane/ dichloropentane conformers are determined.

For semi-empirical calculation, statistical weight matrices were estimated from the conformational energy map of representative small segments of polymer chain by AM1 calculation using HyperChem7. The procedure is as following

- Select a section of PVF and PVC of which conformations depend on two neighboring backbone bond rotation angles were selected. The atom coordinates are adjusted to minimize the energy while the torsion angle is constant.
- The conformational energies for each of these fragments are calculated as a function of the rotation angles and torsion are rotated from 0o to 360° (10° for each step).
- The conformational energy maps are generated and statistical weights are assessed for each of the nine pair-wise dependent rotational states, for example

$$U_{\phi_i, \phi_j} = \frac{\sum_{\phi_i} \sum_{\phi_j} \exp [-V(\phi_i, \phi_j)/RT]}{\sum_{10^\circ}^{360^\circ} \sum_{10^\circ}^{360^\circ} \exp [-V(\phi_i, \phi_j)/RT]} \quad (3.20)$$

where $V(\phi_i, \phi_j)$ is the conformational energy (kcal/mole) at torsional angles ϕ_i and ϕ_j , R is the gas constant, and T is the absolute temperature.

- The RIS estimation for polymer molecules is usually based on the first- and second-order interactions for three rotational isomeric states i.e. trans (t), gauche⁺ (g⁺), and gauche⁻ (g⁻). Then, all the statistical weight matrices assigned to the skeletal bonds are 3x3 dimension.

3.1.4 Monte Carlo Simulation of polymer

In the 1990s, the research group at Akron designed a new high coordination lattice that is appropriate to simulate a real polymer chain at the bulk. This method succeeds in studying the dynamic and static properties of simple structured polymers such as polyethylene, polyoxyethylene, and polypropylene. The lattice simulation techniques for real specific polymers with the characteristics can be described by three steps.

Step 1. Mapping: A fully atomistic model of an amorphous polymer in continuous space is mapped at bulk density onto a coarse-grained representation on a suitable chosen high coordination lattice. The mapping produces a coarse-grained representation of the real chain, so diminishing the number of fundamental particles

in the posterior simulation on the lattice will be computationally effective, even when the system is bulk density.

Step 2. Dynamics/Equilibration: The system develops through time by simulation on the high coordination lattice. Monte Carlo simulation is used with Metropolis criteria for the acceptance of the bead moves. The move must have a change that retains the local conformational characteristics of the real atomistic chains derived in Step 1.

Step 3. Reverse Mapping: The final process gives a fully atomistic explanation of the system in continuous space from randomly chosen points in the trajectory. The reverse mapping must restore chain atoms (and bonds) that were perfunctorily eliminated from the delineation of the system during the mapping in Step 1.

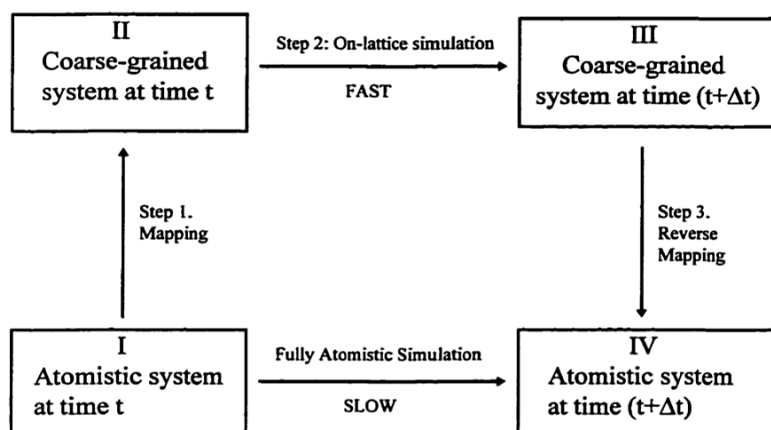


Figure 3.1 Schematic representation of three numbered steps in a MC simulation on a high coordination lattice that replaces a simulation of the fully atomistic system in a continuous space.

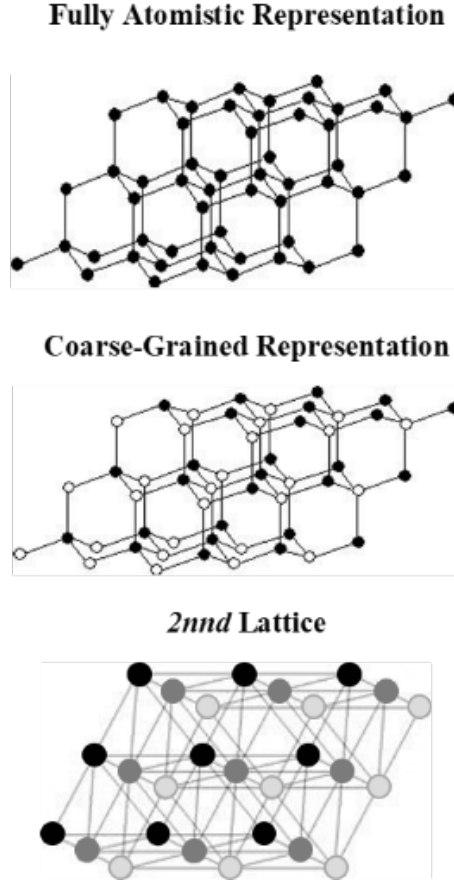


Figure 3.2 Graphical demonstration of how a tetrahedral lattice can be converted into a *2nd* lattice.

For vinyl polymer, the relations between the *2nd* lattice and the underlying diamond lattice can be illustrated as following. The rotational isomeric states of the two C–C bonds to bead j can be assigned obviously, given the vectors from bead i to bead j , and from bead j to bead k . These assignments can be showed in a 12x12 matrix. The 12x12 matrix is used to associate the reverse mapped C–C bonds in positive z direction from each *2nd* bead. This 12x12 matrix can be abbreviated to sixteen 3x3 blocks as follows,

$$\begin{bmatrix} A & B & A & B \\ B & A & B & A \\ A & B & A & B \\ B & A & B & A \end{bmatrix} \quad \text{and} \quad A = \begin{bmatrix} a & b & c \\ c & a & b \\ b & c & a \end{bmatrix} \quad B = \begin{bmatrix} b & c & d \\ c & d & b \\ d & b & c \end{bmatrix} \quad (3.21)$$

where a is tt or g^+g^+ , d is rev or g^-g^- . In all sixteen blocks, b and c are selected from tg^+tg^- , g^+t , g^-t , g^+g^- , g^-g^+ , and col , where col denotes an unphysical collapse.

The long-range interaction involves both long-range intramolecular interaction that separated by more than four bonds and the non-bonded intermolecular interaction. The long-range interactions are gotten from a discretized form of the Lennard-Jones (LJ) potential, in which the second virial coefficient (B_2) for polymers are assessed similar to a nonideal gas using the Mayer f function according to the imperfect gas theory as follows:

$$B_2 = \frac{1}{2} \int \{ \exp[- \beta u(r)] - 1 \} d\mathbf{r} = \frac{1}{2} \int f d\mathbf{r} \quad (3.22)$$

where, $\beta = 1/kT$; k is the Boltzmann constant and f is called the Mayer function. B_2 in the lattice space can be obtained by dividing the integral for each sub-shell as:

$$\begin{aligned} B_2 &= -\frac{1}{2} \left[- \int d\mathbf{r} + \sum_{1st} \int_{cell} f d\mathbf{r} + \sum_{2nd} \int_{cell} f d\mathbf{r} + \sum_{3rd} \int_{cell} f d\mathbf{r} + \dots \right] \\ &= \frac{V_c}{2} \left[1 - \sum_{1st} \langle f \rangle_{1st} - \sum_{2nd} \langle f \rangle_{2nd} - \sum_{3rd} \langle f \rangle_{3rd} - \dots \right] \end{aligned} \quad (3.23)$$

where $\int_{cell} d\mathbf{r}$ is the shell volume V_c of the $2nd$ lattice. The shell averaged $\langle f \rangle$ can be determined by

$$\langle f \rangle = \int_{cell} f d\mathbf{r} / \int_{cell} d\mathbf{r} \quad (3.24)$$

To determine $\langle f \rangle$, the center of the one monomer is fixed at the origin while the others are allowed to be at any lattice sites. Therefore, Eq. (3.23) is transformed to

$$B_2 = \frac{V_c}{2} \left[1 - z_1 \bar{f}_{1st} - z_2 \bar{f}_{2nd} - z_3 \bar{f}_{3rd} - \dots \right] \quad (3.25)$$

where, z_i is the coordination number of the i th shell and the shell interaction parameter, u_i , for the i th neighbor can be equated as

$$\exp(-\beta u_i) - 1 = \bar{f}_{ith} \quad (3.26)$$

In these simulations, the Lennard-Jones (LJ) potential energy function is employed as follows:

$$u = \begin{cases} \infty & r < 2.5 \text{ \AA} \\ u_{\text{LJ}} = 4\epsilon \left[\left(\frac{\sigma}{r} \right)^{12} - \left(\frac{\sigma}{r} \right)^6 \right] & r \geq 2.5 \text{ \AA} \end{cases} \quad (3.27)$$

Here, the LJ-potential parameters for chloroethane ($\epsilon/k_B = 300.0$ K, $\sigma = 4.898$ Å) and fluoroethane ($\epsilon/k_B = 253.3$ K, $\sigma = 4.268$ Å) was used to estimate the interaction at the simulated temperature of 600 K (Poling, 2002) and only the first shell parameters for PVC (21.968, 1.575, -1.369 kJ/mol) and PVF (17.369, 0.330, and -0.776 kJ/mol) were employed to speed up the calculation.

3.1.5 Moves in the Simulation

Two types of moves were recommended into the simulation. One type is a series of moving single beads in which every bead has a chance to move to one of the nearest vacant neighbors within the constraints of the bond length and energy. The movement of a single bead on the 2nd lattice can move the position of either two or three consecutive carbon atoms on the underlying fully atomistic diamond lattice. For the purpose of improvement computational efficiency, a set of multiple bead pivot moves is executed.

Two to six bead pivot moves are applicable in the simulation. For every Monte Carlo Step (MCS), single bead moves and again multiple bead pivot moves are operated randomly. Every bead is tried once, on average, both in single bead moves and pivot moves, respectively. Moves to cause double occupancy and collapses were forbidden. The moves are accepted or rejected according to the Metropolis criterion.

3.1.6 System Description

MC simulations on 2nd lattice were based on coarse-grained chains with 46 monomer $[\text{CH}_2\text{CHX}]$ beads. The bulk systems were composed of 12 chains in the box of $16 \times 16 \times 16$ lattice units (equal to $4 \times 4 \times 4$ nm) equivalent to the density of 1.38 and 1.45 g/cm^3 for PVC and PVF systems which are close to their experimental densities (Lee, 1992; Ludovice, 1992). The simulation temperature was above their melting temperature at 600 K for *atactic* chains with trajectories of 10,000,000 MCS after equilibration.

3.1.7 Fully atomistic models

Reverse mapping of coarse-grained (CG) models from 2nd lattice to atomistic representation in the continuous area can be done by defining the location of central backbone atoms that are demonstrated on the diamond lattice underling the 2nd lattice. After structural relaxation by MC simulation of CG models, all bonds and all the missing atoms will be restored. The coordinates of the carbon, fluoride and hydrogen atoms in polymer chains were generated after reverse mapped back onto the diamond lattice. The side group (X) configuration can be also uniquely in accordance with the description of the RIS model. The atomic structure can then be adjusted off-lattice by reducing the energy of the selected snapshot. This procedure is performed using Xenoview (<http://www.vemmer.org>) with PCFF force field until the gradient is less than 0.1 kcal/(mol Å). The steepest descents method is used if the gradient is greater than 1000 kcal/(mol Å), and the conjugate gradient is used in other ways. In addition, short NVT molecular dynamics (< 1 ns) was run to further relax the atomistic structures. To regularize these atomistic models, some molecular and material features of amorphous polymer structures will be defined and compared with experimental data including conformational statistics and solubility parameter factors.

3.2 Monte Carlo simulation : Effect of chain stiffness on the free surface of polymers

3.2.1 Rotational Isomeric State (RIS) Model

The RIS model (Flory, 1969; Mattice, 1994) is an effective method to calculate quickly by computer the conformational-dependent properties of a single polymer chain based on its molecular structure (bond length, bond angles, and torsion potential energetics) in the matrix multiplication formalism. The calculation is the exact result for the specific model, as imposed by the molecular geometry and the intramolecular interaction energies. From the RIS formalism, the statistical weight matrix of polyethylene-like model can be defined by:

$$U = \begin{bmatrix} 1 & \sigma' & \sigma' \\ 1 & \sigma' & \sigma'\omega' \\ 1 & \sigma'\omega' & \sigma' \end{bmatrix} \quad (3.28)$$

where the statistical weights of the first-, $\sigma = \exp(-E_\sigma/RT)$, and the second-order, $\omega = \exp(-E_\omega/RT)$, interaction parameters are multiplied by the chain stiffness parameter (k) as $\sigma' = k\sigma$ and $\omega' = k\omega$ where the energy parameters of the unperturbed polyethylene are $E_\sigma = 2100$ and $E_\omega = 8400$ J/mol, respectively (Misra, 1995). For this 3x3 matrix, the rows and columns are the conformations of $(i-1)$ th and i th bonds, respectively, with the index of t , g^+ and g^- states (*trans*, *gauche*⁺ and *gauche*⁻ conformation with the torsion angles of 180°, +60° and -60°, respectively).

The conformational partition function (Z) which is the sum over all rotational states of the product of these weights can be determined using the above statistical weight matrices.

$$Z = \prod_i U_i \quad (3.29)$$

The probability of bond i at the rotational isomeric state, η , can be derived by dividing Z into the sum of the statistical weights of all conformations where this bond is in the η state.

$$p_{\eta,i} = \frac{Z_{\eta,i}}{Z} = \frac{U_1 U_2 \dots U_{i-1} U'_{\eta,i} U_{i+1} \dots U_n}{Z} \quad (3.30)$$

where U_i is the statistical weight matrices in the form as shown in Eq (3.30) and $U'_{\eta,i}$ is similar to U_i with the statistical weights of two rows except for the state η of bond i are zero.

The characteristics ratio defined as the proportion of the unperturbed mean square end-to-end distance, $\langle r^2 \rangle_0$, relative to that of the fully flexible chain (nl^2) can be used to describe the chain stiffness at the molecular level.

$$C_\infty = \lim_{n \rightarrow \infty} \frac{\langle r^2 \rangle_0}{nl^2} \quad (3.31)$$

where n and l are the number of internal bonds and the bond length, respectively.

For a particular conformation, the squared end-to-end distance of a polymer chain can be obtained by the matrix multiplication.

$$r^2 = G_1 G_2 \dots G_{n-1} G_n \quad (3.32)$$

The internal G_i matrices have 5x5 dimensions which are in the 3x3 block format.

$$G_i = \begin{bmatrix} 1 & 2l^T T & l^2 \\ 0 & T & l \\ 0 & 0 & 1 \end{bmatrix}, 1 < i < \quad (3.33)$$

Here, l is the bond vector, l^T is its tranpose and T is the transformation matrix defined by

$$l = \begin{bmatrix} l \\ 0 \\ 0 \end{bmatrix} \text{ and } l^T = [l \quad 0 \quad 0]$$

$$T_i = \begin{bmatrix} -\cos\theta & \sin\theta & 0 \\ -\sin\theta\cos\phi & -\cos\theta\cos\phi & -\sin\phi \\ -\sin\theta\sin\phi & -\cos\theta\sin\phi & \cos\phi \end{bmatrix}$$

where θ and ϕ denote the bond angle and the torsion angle, respectively. G_1 and G_n are given by the top row and the last column of G_i , respectively.

The unperturbed mean square end-to-end distance, $\langle r^2 \rangle_0$, is the ensemble average value of all possible conformation and can be calculated as a serial product of $\langle G_i \rangle$ matrices.

$$\langle r^2 \rangle_0 = Z^{-1} G_1 \langle G_2 \rangle \dots \langle G_{n-1} \rangle G_n \quad (3.34)$$

where the super-generator matrix $\langle G_i \rangle$ for the bond vector is determined by

$$\langle G_i \rangle = \begin{bmatrix} U & (U \otimes I^T) \parallel T \parallel & 0 \\ 0 & (U \otimes I^T) \parallel T \parallel & U \otimes I \\ 0 & 0 & U \end{bmatrix}_i$$

where I is the identity matrix and \otimes is denoted the direct product. U_i is of dimensions 3×3 for polyethylene and I_A is of dimensions 4×4 , the direct product, $U_i \otimes I_A$, is of dimensions 12×12 , with the form

$$U_i \otimes I_A = \begin{bmatrix} u_{11}I_A & u_{12}I_A & \cdots \\ u_{21}I_A & u_{22}I_A & \cdots \\ \vdots & \vdots & \ddots \end{bmatrix}$$

The chain stiffness can be checked at the bond and chain scale using the probability of the *trans* state and the characteristics ratio in Eq. (3.30) and (3.34), respectively. The bond probabilities and the characteristic ratios at 473 K with different chain stiffness parameters ($k = 0.0$ to 2.0) calculated by the RIS model and those averaged from MC simulations are presented in Table 3.1 Note that the fractions of

trans determined by the RIS model of a single chain are relatively smaller than those averaged from MC trajectories of polymer surfaces with multiple chains (in the next section).

The probability of *trans* conformation (and the characteristics ratio) of the *polyethylene-like* model is systematically increased from the most flexible chain 2.192 (0.333) to the most rigid chain 8.702 (0.683). The range of the chain stiffness parameter ($0.0 \leq k \leq 2.0$) is suitable in the lattice MC simulation used in this work so that structural relaxation and equilibration can be satisfied to observe different characteristics of polymer surfaces.

Table 3.1 The characteristics ratio and probability of the conformational states with different chain stiffness parameters at 473 K.

k	C_∞	P_t	P_g^+, P_g^-	$*P_t$	$*P_g^+, P_g^-$
0.0	2.192	0.333	0.333	0.393 ± 0.006	0.303 ± 0.007
0.5	4.490	0.494	0.253	0.525 ± 0.006	0.237 ± 0.006
1.0	6.282	0.579	0.211	0.616 ± 0.006	0.192 ± 0.005
1.5	7.548	0.636	0.182	0.687 ± 0.005	0.156 ± 0.005
2.0	8.702	0.683	0.159	0.756 ± 0.005	0.122 ± 0.005

*determined from MC simulation.

3.2.2 Monte Carlo simulation

MC simulation of *polyethylene-like* models has been proposed and applied to study polymer-blend nanofilm (Sirirak, 2023), random copolymer surface (Wichai, 2021), and polymer crystallization (Sirirak, 2023). In this work, the *polyethylene-like* model is used to mimic the characteristics of chain stiffness (Sirirak, 2023). Polymers are coarse-grained, as one monomer unit to one CG bead, and mapped onto the *2nd* lattice where the conformation of C-C bonds can be defined implicitly from the underlying diamond lattice (Baschnagel, 2000). The *on-lattice* intra- and intermolecular interaction of *polyethylene-like* chains are treated by the refined RIS model (Flory, 1969; Mattice, 1994) and the discretized version of LJ potential energy, respectively

(Cho, 1997). The statistical weight matrix for *polyethylene-like* chains (U_{PE}) can be transformed to the lattice version (U_{2nd}) as (Baschnagel, 2000):

$$U_{PE} = \begin{bmatrix} 1 & \sigma' & \sigma' \\ 1 & \sigma' & \sigma'\omega' \\ 1 & \sigma'\omega' & \sigma' \end{bmatrix} \rightarrow U_{2nd} = \begin{bmatrix} 1 & 4\sigma' & 2\sigma'\sigma'(1+\omega') \\ 1 & 4a & 2b\sigma'(1+\omega') \\ 1 & 4b & 2c(1+\omega') \end{bmatrix} \quad (3.35)$$

The first- ($\sigma' = k\sigma$) and the second-order ($\omega' = k\omega$) interaction parameters for *polyethylene-like* chains are defined by Eq. (3.28), with $a = \sigma'\omega'^{1/8}$, $b = \sigma'\omega'^{1/4}$ and $c = \sigma'^2\omega'^{1/2}$. For *polyethylene-like* models used in this work, polymers can be considered as stiffer chains ($k = 1.5$ and 2.0) or more flexible ($k = 0.0$ and 0.5) than the normal PE ($k = 1.0$).

Non-bonded intermolecular interaction between two CG beads can be treated by the Lennard-Jones (LJ) potential energy with $\sigma = 0.44$ nm and $\epsilon/k = 185$ K for ethylene (Poling, 2000). The first three shell of intermolecular energies on the *2nd* lattice (with cut-off radius = 0.75 nm) at 473 K are $u_1 = 15.048$, $u_2 = 0.620$ and $u_3 = -0.625$ kJ/mol, respectively.

The starting configurations of chains on the lattice were based on the self-avoiding walks in the simulation box. After that, intra- and intermolecular energies were included. Single-bead move was used to displace the CG beads to the empty position in the lattice. Each single-bead move corresponds to the displacement of two or three carbon atoms in the fully atomistic representation of the chain (Baschnagel, 2000). The acceptance of each bead move is governed by total (RIS + LJ) energy change according to the Metropolis rule. Monte Carlo Step (MCS) is assigned as a set of bead movements that are randomly tried once, by average.

3.2.3 Free surface formation

The technique to create the free surface of polymer melts is explained in our recent publications (Vao-soongnern, 2021; Wichai, 2021; Sirirak, 2023). In this work, all the systems were created as free-standing thin films with two polymer-vacuum surfaces made of 56 *polyethylene-like* chains with 50 repeating units. The starting box dimension of 25×25×25 units was first used to create and equilibrate the bulk structures. Then, the periodic box in the z direction was extended 3 times to 75 units so that the periodic structures could not interact with their parent chains. Free-standing

thin films can be obtained to represent the model for the polymer-vacuum surface of polymer melts.

All simulations were performed at 473 K which was higher than the melting (T_m) and glass transition temperature (T_g) of normal ($k = 1.0$) polyethylene to facilitate comparison with the results to previous reports (Doruker, 1998; Vao-soongnern, 1999 and 2001). In addition, all *polyethylene-like* chains with different chain stiffness parameters are in the molten state at 473 K (Sirirak, 2023). As T_g is related to the temperature at which the local segment of polymer chains starts to move motion, it is expected that T_g should be increased for stiffer chains. Nevertheless, the main focus of this work is to study the molecular and structural properties of the free surface of polymer melts. The study about glass transition temperature for polymers with different chain stiffness is also interesting and would be investigated in the future.

3.3 The effect of intermolecular interaction on polymer crystallization

For all simulations, there were 38 chains of *PE-like* molecules with 24 monomer units in each system. These CG chains were created so that one bead was represented by one ethylene (CH_2CH_2) unit and then mapped to the second nearest neighbor diamond ($2nnd$) lattice, a distorted cubic lattice ($\alpha = \beta = \gamma = 60^\circ$) derived from removing every other position on the underlying diamond lattice. The $2nnd$ lattice has a coordination number of 12, similar to the closest packing of uniform hard spheres, and is suitable for mapping the CG model of several polymers (Baschnagel, 2000; Xu, 2002; Vao-soongnern, 2004 and 2023; Wichai, 2021; Jamornsuriya, 2022; Kusinram, 2022; Sirirak, 2023). All CG chains were put in the simulation box with a length of 16 units (equivalent to 4.0 nm). The bead occupancy (total number of CG beads divided by box volume) in the $2nnd$ lattice was fixed to 0.225 (comparable to the density = 0.95 g/cm³) which is close to the density of crystalline PE (Xu, 2001).

For CG *PE-like* models, the RIS model (Mattice, 1994) and the LJ potential energy were adopted to describe the intra- and intermolecular interactions in bulk polymers, respectively (Cho, 1997). The original RIS statistical weight matrix of the PE chain (U_{PE}) is formulated to the CG model on the $2nnd$ lattice (U_{2nnd}) according to (Baschnagel, 2000):

$$U_{PE} = \begin{bmatrix} 1 & \sigma & \sigma \\ 1 & \sigma & \sigma\omega \\ 1 & \sigma\omega & \sigma \end{bmatrix} \rightarrow U_{2nd} = \begin{bmatrix} 1 & 4\sigma & 2\sigma\sigma(1+\omega) \\ 1 & 4a & 2b\sigma(1+\omega) \\ 1 & 4b & 2c(1+\omega) \end{bmatrix} \quad (3.36)$$

Here, two statistical weights are defined as $\sigma = \sigma_0 \exp(-E_\sigma/k_B T)$ and $\omega = \omega_0 \exp(-E_\omega/k_B T)$ with $E_\sigma, E_\omega = 2100, 8400$ J/mol (Abe, 1965), respectively, and $a = \sigma\omega^{1/8}$, $b = \sigma\omega^{1/4}$ and $c = \sigma^2\omega^{1/2}$ and k_B is Boltzmann's constant,

To investigate the influence of intermolecular interaction between polymer chains, the original non-bonded interaction LJ parameters for the CG model of PE beads ($\sigma = 0.44$ nm and $\varepsilon/k = 185$ K) were varied in the range of ($125 \text{ K} \leq \varepsilon/k \leq 205 \text{ K}$) with the same bead diameter ($\sigma = 0.44$ nm). For *PE-like* models with ($125 \text{ K} \leq \varepsilon/k < 185 \text{ K}$) or ($185 \text{ K} < \varepsilon/k \leq 205 \text{ K}$), CG beads in polymer chains can be regarded as more repulsive or more attractive interaction than those in the normal PE ($\sigma = 0.44$ nm and $\varepsilon/k = 185$ K). In this work, five *PE-like* chains with different intermolecular interaction parameters ($\sigma = 0.44$ nm and $\varepsilon/k = 125, 145, 165, 185$, and 205 denoted by E125, E145, E165, E185, and E205, respectively) were used for comparison.

The starting configurations of the CG model of *PE-like* chains in the periodic box were created via self-avoiding random walks. After that, the intra- and intermolecular energetics were applied in the simulation. *PE-like* chains were randomly displaced on the *2nd* lattice by the single-bead movement to the vacant lattice sites. The Metropolis criteria were adopted to accept or reject the moves from the changes in total energetics in every bead displacement. On average, one Monte Carlo Step (MCS) is counted when every bead randomly tries to change its position. The single bead move on the *2nd* lattice corresponds roughly to the random local configuration changes that happen in a real polymer system due to jumps from one minimum of the torsion potential to the next one. Thus, the MCS in this dynamic MC simulation can be potentially mapped to the real time such as done previously with MD simulation [70]. The structure formation at an early stage was monitored with stepwise cooling from the molten state for the total 100 million MCS trajectories, ($473 \text{ K} \rightarrow 400 \text{ K} \rightarrow 350 \text{ K} \rightarrow 298 \text{ K}$ with 10 million MCS in each step except the final one with 70 million MCS). Data analysis was done for structures saved every 10,000 MCS from simulation trajectories. The crystallization temperature (298 K) was significantly higher

than T_g of normal PE (ca. 150 K) such that the crystallization can be observed within reasonable simulation time.

All simulations were performed at the same density (0.95 g/cm^3) with the same chain length (24 CG beads) and chain number (38 chains) in all systems so that the effect of intermolecular interaction on crystallization can be better realized although the actual densities should be depend on the intermolecular interaction. Three independent runs were repeated. The chain length of 24 monomers is slightly larger than the box dimension of 16 units so that the ordered structure can be formed as a single domain with all chains oriented in the same direction. Although the densification is produced by cooling, the neglect of densification should mostly to delay the onset of crystallization in the simulation. Like the setup in our recent publication (Jamornsuriya, 2022; Sirirak, 2023; Vao-soongnern, 2023), the systems were stepwise cooled from 473K (well above the melting temperature) to 298 K which is about 70 K below melting temperature of this normal PE model ($\sigma = 0.44 \text{ nm}$ and $\epsilon/kT = 185 \text{ K}$). Although the actual trajectories in each run are different, the overall characteristics are more or less the same. Thus, only one representative trajectory with 100 million MCS is presented in this work.

3.4 Molecular dynamics (MD) simulation of detailed structures and ion transportation of polymerized ionic liquid/ionic liquid blends

3.4.1 Experimental Methods

3.4.1.1 Materials

1-vinylimidazol,1-butyl-3-methylimidazolium bis(trifluoromethanesulfonyl)imide (Bmim-TFSI) and lithium bis(trifluoromethanesulfonyl)imide (Li-TFSI) were purchased from Tokyo Chemical Industry Co. Ltd. 1-bromobutane, methanol, dimethylformamide (DMF), acetone, silver nitrate (AgNO_3), toluene and 2,2'-azobis(isobutyronitrile) (AIBN) were purchased from FUJIFILM Wako Pure Chemical Corporation.

3.4.1.2 Synthesis of Poly (1-butyl-3-vinylimidazolium bromide)

1-vinylimidazole (157.2 g, 1.67 mol) and 1-bromobutane (256 g, 1.87 mol) were dissolved in methanol (150 mL) and refluxed at 65 °C for 3 days. Methanol and unreacted 1-bromobutane are removed from the products under vacuum. Purity of the product was ascertained with ^1H NMR. The product 1-butyl-3-vinylimidazolium bromide (356.5 g, 1.54 mol) and AIBN (7.66 g, 0.0467 mol) as initiator were dissolved in water (200 mL) and polymerized at 60 °C for 18 h. The polymer was dialyzed against water for 1 week using a dialysis tube. During the dialysis, the water was refreshed daily. The resultant solution was dried via a freeze-drying method and poly (1-butyl-3-vinylimidazolium bromide) was obtained in a powder form (62.5 g, 17.5 % yield).

3.4.1.3 Synthesis of Poly (1-butyl-3-vinylimidazolium bis(trifluoromethanesulfonylimide))

Poly (1-butyl-3-vinylimidazolium bromide) (24.9 g, 0.108 mol) was dissolved in water (600 mL). Li-TFSI (37.7 g, 0.131 mol) was dissolved in water (220 mL). While stirring the poly (1-butyl-3-vinylimidazolium bromide) solution, the Li-TFSI solution was dropped into the stirring solution. After dropping, the mixed solution was stirred at room temperature for 3 days. The precipitation was filtered and washed with water. AgNO_3 aqueous water was dropped into the filtrate. 41.6 g of poly (1-butyl-3-vinylimidazolium bis(trifluoromethane-sulfonylimide)) was obtained (89.2 % yield). The white liquid of Bvim-TFSI was obtained and confirmed the structure by the NMR method (NMR JNM ECS-400, JEOL Ltd., Tokyo, Japan). Figure 3.4.1 shows the ^1H -NMR result of Bvim-TFSI in CDCl_3 solvent. The board and sharp peak at each position shown the unreacted monomer molecules were completely removed from the polymer product.

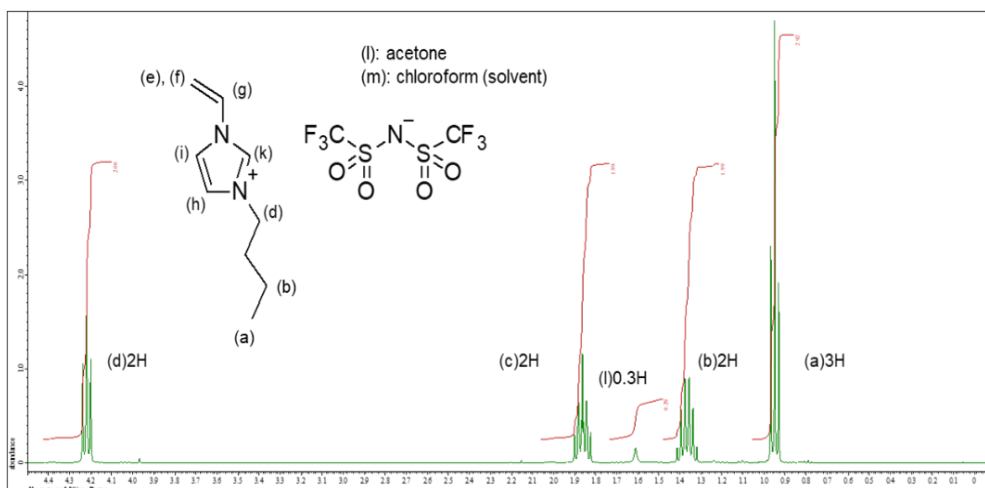


Figure 3.3 NMR spectra of Bvim-TFSI.

3.4.1.4 Synthesis of blend systems: [Pbvim-TFSI]-[Bmim-TFSI]

For Low polymer concentrations (from 10 wt% to 30 wt%): Suitable amounts of poly (1-butyl-3-vinylimidazolium bis(trifluoromethanesulfonylimide)) was added to Bmim-TFSI and the polymer was completely dissolved.

For High polymer concentrations (from 40 wt% to 95 wt%): Suitable amounts of poly (1-butyl-3-vinylimidazolium bis(trifluoromethanesulfonylimide)) and Bmim-TFSI were dissolved in acetone and mixed. Acetone was removed from the mixed solution under vacuum.

3.4.1.5 Characterization

3.4.1.5.1 Differential Scanning Calorimetry (DSC)

The glass transition temperature (T_g) of Pbvim-TFSI with various Bmim-TFSI concentrations was determined by DSC using a DSC 8230 (Rikaku Instruments Inc., Tokyo, Japan). The sample films were prepared around 10-20 mg in the aluminum pan. The pans were hermetically sealed and drying in the vacuum before DSC measurement. Samples were conditioned at a temperature range of -120 °C to 100 °C for three cycles with heating and cooling rates of 10 K/min.

3.4.1.5.2 Ionic Conductivity Measurement: Broadband Dielectric Spectroscopy (BDS)

The ionic conductivity was determined by Novocontrol high-resolution alpha-A dielectric analyzer (Novocontrol Technologies GmbH & Co. KG, Montabaur, Germany) with a frequency range from 1.0×10^{-1} to 1.0×10^6 Hz. The sample liquids were dried in vacuum and then they bring into a sample cell of diameter 14 mm. and spacer 0.17 mm. thickness at 100 °C overnight. The conductivity values were measured under nitrogen conditions with temperatures ranging from -100 °C to 180 °C, the temperature ranges were controlled using a Cryogenic temperature controller (Model 331 cryogenic temperature controller, Lake Shore Cryotronics Inc., Ohio, USA).

3.4.2 Molecular dynamics simulation

3.4.2.1 Simulation details

Molecular dynamics simulations were performed using the open-source GROMACS 2020.1 package (Abraham, 2020). The OPLS-AA force field and non-bond parameters of poly (1-butyl-3-vinylimidazolium bis(trifluoromethanesulfonyl)imide): Pbvim-TFSI were directly obtained from (Jorgensen, 1996; Doherty, 2017; Keith, 2017; Mogurampelly, 2017). The optimized structures of Pbvim⁺ with 15 monomers were generated using PolyPargen web server (Yabe, 2019). The structure and the force field parameters of ionic liquid (1-butyl-3-methyl-imidazolium bistriflimide): Bmim-TFSI were directly obtained from Acevedo and co-workers' works (Acevedo, 2018).

For constructing the polyIL material, 20 atomistic polymer chains (15 monomers each) created from the above equilibration procedure are packed into a simulation box (using the cubic cell with periodic boundary conditions) with corresponding number of TFSI⁻ anions and Bmim⁺ cations (Zhang, 2020), (as listed in Table 3.2). The initial box length is 10 nm.

Table 3.2 Composition Details of PolyIL–IL Blend Electrolytes with Varying ILs Loadings.

$C_{\text{Bmim-TFSI}}$	PolyILs			ILs	
	Bvim ⁺	Pbvim ⁺	TFSI ⁻	Bmim ⁺	TFSI ⁻
0.0	300	20	300	0	0
0.2	300	20	300	60	60
0.4	300	20	300	120	120
0.6	300	20	300	180	180
0.8	300	20	300	240	240
1.0	0	0	0	300	300

Equations of motion in MD simulations were integrated using the leapfrog algorithm with a time step of 1 fs. Temperature was controlled using a V-rescale thermostat with a relaxation time of 1 ps. A Parrinello-Rahman barostat (coupling time 1 ps with an isothermal compressibility of $4.5 \times 10^{-5} \text{ bar}^{-1}$) was employed for constant pressure simulations. Electrostatic interactions were calculated using particle mesh Ewald with a real-space cutoff of 1.3 nm. Lennard-Jones interactions were truncated at 1.3 nm, with long-range corrections for both potential and pressure applied. Neighbor lists were updated every 10-time steps using a list cutoff radius of 1.3 nm (Zhang, 2020). Bond constraints were solved using the Linear Constraint Solver (LINCS) algorithm (Khongvit, 2020).

3.4.2.2 Simulation procedure

Such a pre-equilibrium procedure was inspired by the 25-step decompression. And then a multi-step equilibration procedure was used to prepare the equilibrated configuration for the production run follow as: The first step, using 0.1 ns NVT simulation at 1000 K and 0.1 ns. The second step, using 0.1 NPT simulation at 600 K and 100 bar. The third step, 0.1 NPT simulation at 600 K and 1 bar, all 3 steps use 10 steps. The equilibrated system was finally step to an NPT production run for 110 ns for in-depth analyses (Zhang, 2020). And All images were created using VMD open-source software (Humphrey, 1996). This process resulted in an equilibrated structure with box size and density for each system reported in Table 3.3.

Table 3.3 Box size, density (ρ), radius of gyration (R_g), and average end to end distance (R_{ee}) of PolyIL–IL Blend Electrolytes with Varying ILs Loadings.

$C_{\text{Bmim-TFSI}}$	Box size (nm ³)	ρ (g/cm ³)	R_g (nm)	R_e (nm)
0.0	5.41 ³	1.375	0.357	0.706
0.2	5.78 ³	1.343	0.334	0.646
0.4	6.09 ³	1.329	0.318	0.605
0.6	6.37 ³	1.312	0.308	0.580
0.8	6.65 ³	1.300	0.301	0.559
1.0	5.60 ³	1.200	0.257	0.417

3.4.2.1 Quantification Measures

3.4.2.1.1 Validated method for equilibrium: potential, density and radius of gyration (R_g)

Polymer conformation was investigated in terms of the radius of gyration (R_g) and the average end-to-end distance (R_{ee}). The R_g is calculated as follows:

$$R_g = \left(\frac{\sum_i \|r_i\|^2 m_i}{\sum_i m_i} \right)^{\frac{1}{2}} \quad (3.37)$$

where m_i is the mass of atom i and r_i is the position of atom i with respect to the center of mass of the molecule (Khongvit, 2020).

3.4.2.1.2 Polymer dynamics

3.4.2.1.2.1 The mean squared displacement (MSD) and Diffusion coefficient (D)

The dynamics of polymer chains were studied both in terms of translational and orientational mobility. Translational dynamics were analyzed through a time-dependent diffusion coefficient (D), derived from the mean squared displacement (MSD) using the Einstein relation (Allen, 1987);

$$\lim_{t \rightarrow \infty} \langle \|r_i(t) - r_i(0)\|^2 \rangle = 6Dt \quad (3.38)$$

where $r_i(t)$ and $r_i(0)$ are the positions of the particle at time 0 and t , respectively. The term in the bracket $\langle \dots \rangle$ represents the MSD of the particle.

For the anion (TFSI⁻), the nitrogen atom is used as the reference to calculate the MSD, whereas, for cation 1-butyl-3- methyl-imidazolium (BmIm⁺), the nitrogen atom that connects the butyl functional group was used to calculate the MSD. Polycation diffusivities are not facile to achieve for longer polymer chains (Zhang, 2020). Therefore, in the current study, we overpass the diffusivity of polycations in the polyIL system.

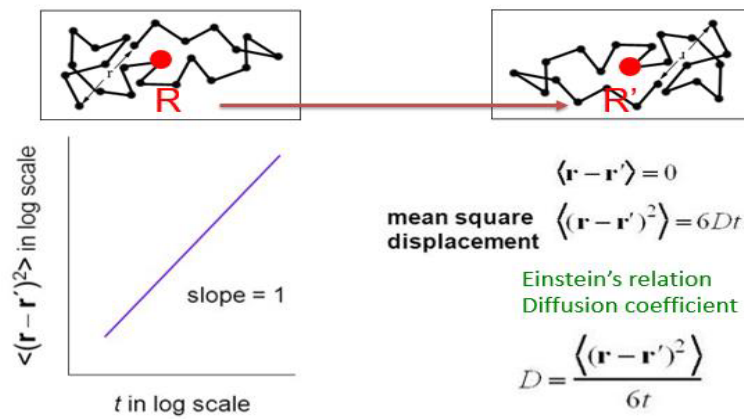


Figure 3.4 The definition of the mean squared displacement (MSD) and Diffusion coefficient (D).

3.4.2.1.2.2 The Orientational autocorrelation functions (ACF)

ACF of PolyIL-IL blends were analyzed through the autocorrelation function (the second Legendre polynomial) of a vector connecting two next-nearest atoms in the backbone of the polymer chains (1-3 vector). The autocorrelation function is calculated through (Khongvit, 2020).

$$P_2(t) = \left\langle \frac{v(t+t_0) \cdot v(t_0)}{|v(t+t_0)| |v(t_0)|} \right\rangle \quad (3.39)$$

where v is the 1-3 vector and the bracket $\langle \dots \rangle$ denotes an average over different time origins t_0 as well as for the 1-3 vectors belonging to the same chain. This function measures the decorrelation of the vector at time $(t + t_0)$ with reference to its position at time t_0 .

We forecasted the local characteristic relaxation times of polymer chains by fitting the Kohlrausch Williams-Watts (KWW) stretched-exponential function (Graham, 1970).

$$f(t) = A \exp(-(t/\tau_{KWW})^\beta) \quad (3.40)$$

where the prefactor A denotes the initial, very fast relaxation (e.g., bond and angle vibrations) and is smaller than unity. The τ_{KWW} stands for the KWW relaxation time and gives an estimation of the characteristic decorrelation time for the 1-3 vector. The stretching exponent β describes deviations from the single-exponential behavior, that is, the behavior typical for a system with only one relaxation time (where $\beta = 0.82$).

3.4.2.1.3 Transference number

The transference number amounts the current transported by the identity of attention (in our case, the anion) relative to the whole current. While a number of definitions of transference number exist, in the current factor, we employ the definition that only depends on ion mobilities and the number of mobile species (Mogurampelly, 2018):

$$t_- = \frac{N_{TFSI^-} D_{TFSI^-}}{N_{TFSI^-} D_{TFSI^-} + N_{BMIM^+} D_{BMIM^+}} \quad (3.41)$$

In pure polyLLs, the cations can be approximated as almost immobile at the temperatures probed in our simulations.

3.4.2.1.4 Glass transition temperature (T_g)

T_g is one of the most essential characteristics of polymers as it describes the plastic normality of these materials at their serve temperature. Glass transition temperature is determined as the temperature at which the specific volume (V_{specific}) of the polymer undergoes a sudden transformation throughout the cooling down procedure (Zhang, 2007; Khongvit, 2016). The T_g determination for each system was started with the final structure obtained from the production run. We use cooling rate $= 1 \times 10^{10}$ K/s and the system density was calculated from the last 1ns from 2ns of NPT trajectory (Mogurampelly, 2017).

Data points corresponding to the glassy and rubbery regimes were separately fitted to two linear regression equations. The point of intersection was then used to denote the T_g .

3.4.2.1.5 Radial Distribution Functions and Coordination Number (RDF&CN)

The structural properties of the monomeric IL, polyIL systems and polyIL-IL blends were evaluated by calculating the pair distribution functions using were identified by calculating the Radial Distribution Functions function (Zhang, 2020),

$$g_{ij}(r) = \frac{V}{4\pi r^2 N_i N_j} \langle \sum_i^{N_i} \sum_j^{N_j} \delta(r - r_{ij}) \rangle \quad (3.42)$$

Where N_i and N_j are the number of atoms of ion species i and j . V is the volume of simulation box, and δ is the Dirac delta function.

3.4.2.1.6 Ideal ionic conductivity

The ionic conductivity of the IL ions, σ , can be determined from

$$\sigma = \lim_{t \rightarrow \infty} \frac{e^2}{6tV k_B T} \langle \sum_i \sum_j q_i q_j \times [R_i(t) - R_i(0)] [R_j(t) - R_j(0)] \rangle \quad (3.43)$$

Where q_i is charge of ion i , e is electronic charge, V is volume of the simulation box, k_B is Boltzmann's constant, T is the absolute temperature, and $\langle \dots \rangle$ represents the ensemble average (Mogurampelly, 2018).

From the cross-correlation term is small and hence may be neglected. As a result, we arrive at a modified Nernst-Einstein equation based exclusively on the free ions (Feng, 2019):

$$\sigma_{NE,modified} = \frac{1}{V k_B T} (q_+^2 D_+ N_+ p_+ + q_-^2 D_- N_- p_-) \quad (3.44)$$

Where D_+ (D_-) and N_+ (N_-) are the diffusion coefficient and the number of cations (anions), respectively, p_+ and p_- are fractions of cations and anions in the free state.